

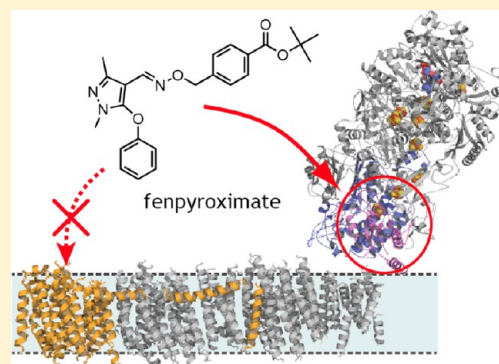
# Fenpyroximate Binds to the Interface between PSST and 49 kDa Subunits in Mitochondrial NADH-Ubiquinone Oxidoreductase

Yusuke Shiraishi,<sup>†</sup> Masatoshi Murai,<sup>†</sup> Naoto Sakiyama,<sup>†</sup> Kentaro Ifuku,<sup>‡</sup> and Hideto Miyoshi<sup>\*,†</sup>

<sup>†</sup>Division of Applied Life Sciences, Graduate School of Agriculture, and <sup>‡</sup>Division of Integrated Life Science, Graduate School of Biostudies, Kyoto University, Sakyo-ku, Kyoto 606-8502, Japan

## Supporting Information

**ABSTRACT:** Using a photoaffinity labeling technique, Nakamaru-Ogiso et al. demonstrated that fenpyroximate, a strong inhibitor of bovine heart mitochondrial NADH-ubiquinone oxidoreductase (complex I), binds to the ND5 subunit [Nakamaru-Ogiso, E., et al. (2003) *Biochemistry* 42, 746–754]. Considering that the main body of the ND5 subunit composed of transmembrane helices 1–15 is located at the distal end of the membrane domain [Efremov, R. G., et al. (2010) *Nature* 465, 441–445], however, their result may be questionable. Because establishing the number and location of inhibitors and/or quinone binding sites in the membrane domain is necessary to elucidate the function of the enzyme, it is critical to clarify whether there is an additional inhibitor and/or quinone binding site besides the interface between the hydrophilic and membrane domains. We therefore performed photoaffinity labeling experiments using two newly synthesized fenpyroximate derivatives [<sup>125</sup>I]-4-azidophenyl fenpyroximate ([<sup>125</sup>I]APF) and [<sup>125</sup>I]-3-azido-5-iodobenzyl fenpyroximate ([<sup>125</sup>I]AIF)] possessing a photoreactive azido group at and far from the pharmacophoric core moiety, respectively. Doubled sodium dodecyl sulfate–polyacrylamide gel electrophoresis revealed that [<sup>125</sup>I]APF and [<sup>125</sup>I]AIF bind to the PSST and 49 kDa subunits, respectively. Careful examination of the fragmentation patterns of the labeled PSST and 49 kDa subunits generated by limited proteolysis indicated that the residues labeled by [<sup>125</sup>I]APF and [<sup>125</sup>I]AIF are located in the Ser43–Arg66 (PSST) and Asp160–Arg174 (49 kDa) regions, respectively, which face the supposed quinone-binding pocket formed at the interface of the PSST, 49 kDa, and ND1 subunits. We conclude that fenpyroximate does not bind to the distal end of the membrane domain but rather resides at the interface between the two domains in a manner such that the pharmacophoric pyrazole ring and side chain of the inhibitor orient toward the PSST and 49 kDa subunits, respectively. This study answers a critical question relating to complex I.



The proton-pumping NADH-ubiquinone oxidoreductase (complex I) couples the transfer of two electrons from NADH to ubiquinone with the translocation of four protons across the membrane that drives energy-consuming processes such as ATP synthesis.<sup>1,2</sup> Complex I is the largest of the multisubunit respiratory chain enzymes. The enzyme from bovine heart mitochondria is composed of 45 different subunits with a total molecular mass of ~1 MDa.<sup>3</sup> The crystal structure of the hydrophilic domain (peripheral domain) of complex I from *Thermus thermophilus* was determined at a resolution of 3.3 Å, revealing the subunit arrangement and the putative electron transfer pathway.<sup>4</sup> Recently, the structures of the entire complex I from *T. thermophilus*<sup>5</sup> and *Yarrowia lipolytica*<sup>6</sup> were determined at 4.5 and 6.3 Å, respectively. As expected from electron microscopic studies, the enzyme is L-shaped with a membrane domain and a hydrophilic domain. However, information about the contact between the two domains, thought to be critical for the function of the enzyme and to form a large binding pocket for quinone/inhibitors,<sup>2,5,6</sup> is still highly limited because the structure in this region has not yet been resolved.

Detailed studies of the action mechanism of specific inhibitors of complex I are helpful for obtaining structural and functional clues about ubiquinone reduction and proton translocation in the enzyme.<sup>1,2,7</sup> In particular, photoaffinity labeling studies using photoreactive derivatives of complex I inhibitors have provided valuable insights into the binding sites of the inhibitors and/or ubiquinone.<sup>8–15</sup> Earlier photoaffinity labeling studies, except the study using a fenpyroximate derivative,<sup>10</sup> indicated that the binding sites of inhibitors reside at the interface between the hydrophilic and membrane domains, including the 49 kDa, PSST, and ND1 subunits. Notably, we recently suggested that the third matrix side loop of the ND1 subunit interacts with the N-terminal (Asp41–Arg63) region of the 49 kDa subunit.<sup>15</sup> Extensive mutagenesis studies using yeast *Y. lipolytica* complex I indicated that the reduction of ubiquinone by electrons from the Fe–S cluster N2 may occur in the large pocket composed of the 49 kDa and

Received: January 12, 2012

Revised: February 14, 2012

Published: February 21, 2012

PSST subunits, though specific binding sites for ubiquinone and different inhibitors may not be identical.<sup>16,17</sup> Thus, the interfacial region of the hydrophilic and membrane domains is considered to be a hot spot for the binding of inhibitors and/or ubiquinone.

Fenpyroximate, whose target site is the mitochondrial complex I of mites, has been used as an acaricide. Using a photoaffinity labeling technique, Nakamaru-Ogiso et al.<sup>10</sup> demonstrated that a fenpyroximate derivative [<sup>3</sup>H]TDF (Figure 1) binds to the ND5 subunit, the largest subunit in

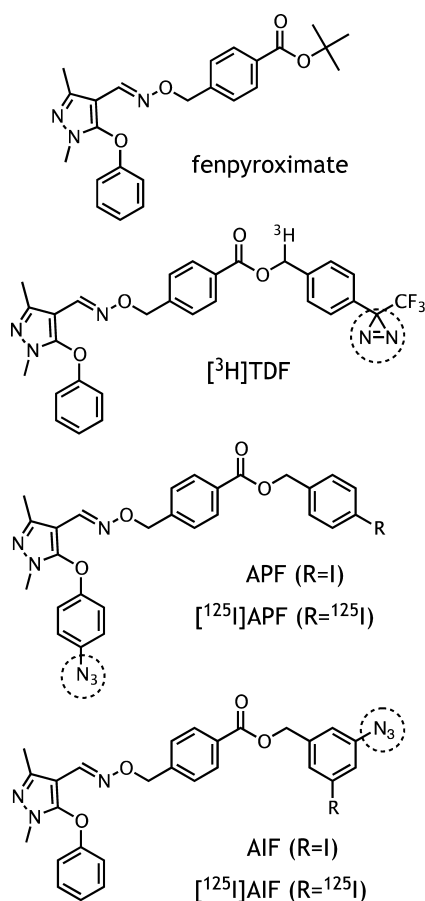


**Figure 1.** Structures of the test compounds used in this study. Photolabile groups (diazirine and azido) are denoted with dashed circles.

the membrane domain. If a wide variety of complex I inhibitors bind to distinct but overlapping regions within a common binding domain<sup>18</sup> (subsequent studies from different laboratories have supported this idea<sup>9,13,14</sup>), their finding seems questionable because the main body of the ND5 subunit (i.e., TM helices 1–15 of Nqo 12 in *T. thermophilus*) is located at the distal end of the membrane domain, far from the hydrophilic domain.<sup>5</sup> When the work by Nakamaru-Ogiso et al.<sup>10</sup> was published, the location of the ND5 subunit had been debated. Nevertheless, they proposed that if the ND5 subunit is located at the distal end of the membrane domain, some segment of the subunit might be close to the interface with the hydrophilic arm because the 49 kDa subunit was also labeled, albeit slightly, by [<sup>3</sup>H]TDF.<sup>10</sup> In this context, it is worth noting that a long amphipathic  $\alpha$ -helix of the Nqo12 subunit of *T. thermophilus* runs along almost the entire length of the membrane domain,<sup>5</sup> although the extension of the  $\alpha$ -helix

seems to end with the 16th transmembrane helix in the vicinity of the Nqo7/10/11 bundle (ND3/6/4L in bovine) and not to reach to the contact region of the hydrophilic [Nqo4 (49 kDa) and Nqo6 (PSST)] and membrane [Nqo8 (ND1)] domains. When considering the study by Nakamaru-Ogiso et al.,<sup>10</sup> it should be realized that a photoreactive diazirine group is attached far from the pharmacophoric pyrazole ring of [<sup>3</sup>H]TDF (see Figure 1), which might hamper any unambiguous interpretation of the result, as discussed previously.<sup>13</sup> Taken together, it remains to be determined whether fenpyroximate indeed binds to the main body of the ND5 subunit. Clarification of this issue is critical for elucidating the function of the membrane domain because it is closely related to the possible occurrence of an additional binding site for inhibitors and/or ubiquinone in the distal (from the hydrophilic domain) end of the membrane domain besides the interfacial region of the PSST, 49 kDa, and ND1 subunits.<sup>1,2</sup> In fact, the report by Nakamaru-Ogiso et al.<sup>10</sup> has been cited as evidence that supports such a possibility (e.g., refs 19–23). We note that the most recent crystal structure of the membrane domain of the *Escherichia coli* enzyme does not suggest any potential site for the binding of quinone in the NuoL, NuoM, and NuoN subunits.<sup>24</sup>

In this study, we conducted the photoaffinity labeling experiments using two newly synthesized fenpyroximate derivatives [[<sup>125</sup>I]-4-azidophenyl fenpyroximate ([<sup>125</sup>I]APF) and [<sup>125</sup>I]-3-azido-5-iodobenzyl fenpyroximate ([<sup>125</sup>I]AIF)] possessing a photoreactive azido group at and far from the pharmacophoric moiety, respectively (Figure 1). Our results clearly revealed that fenpyroximate does not bind to the distal end of the membrane domain but rather resides at the interfacial region between the hydrophilic and membrane domains in a manner such that the pyrazole ring and side chain moiety orient to the PSST and 49 kDa subunits, respectively. This study resolved a critical issue regarding complex I, improving our understanding of the function of the membrane domain.

## EXPERIMENTAL PROCEDURES

**Materials.** Bullatacin and piericidin A were kindly provided by J. L. McLaughlin (Purdue University, West Lafayette, IN) and S. Yoshida (The Institute of Physical and Chemical Research, Yokohama, Japan), respectively. The rabbit anti-*Parracoccus* Nqo6 (bovine PSST homologue) antibody was a generous gift from T. Yagi (The Scripps Research Institute, La Jolla, CA). Protein standards (Precision Plus Protein standards and Kaleidoscope Polypeptide Standards) for SDS–PAGE were purchased from Bio-Rad (Hercules, CA). [<sup>125</sup>I]NaI was purchased from Perkin-Elmer (Waltham, MA). Other reagents were all of analytical grade.

**Synthesis of [<sup>125</sup>I]APF and [<sup>125</sup>I]AIF.** The procedures used to synthesize APF and AIF and their <sup>125</sup>I-labeled derivatives ([<sup>125</sup>I]APF and [<sup>125</sup>I]AIF, respectively) are described in the Supporting Information. The radiochemical yields from the initial [<sup>125</sup>I]NaI were 59–66%, and the specific radioactivities were ~2000 Ci/mmol. Radiochemical purity was examined by HPLC and determined to be >99%.

**Preparation of Bovine SMP and General Procedures for Photoaffinity Labeling.** Submitochondrial particles (SMP) were prepared from isolated bovine heart mitochondria by the method of Matsuno-Yagi and Hatefi<sup>25</sup> and stored in a buffer containing 250 mM sucrose and 10 mM Tris-HCl (pH 7.4) at –80 °C until they were used. NADH oxidase and

NADH-Q<sub>1</sub> oxidoreductase activities in SMP were measured according to procedures described previously.<sup>11,13</sup>

SMP (0.6–1.0 mg of protein/mL, 100  $\mu$ L in a 1.5 mL Eppendorf tube) were incubated with [<sup>125</sup>I]APF or [<sup>125</sup>I]AIF (6–15 nM) in a buffer containing 250 mM sucrose, 1 mM MgCl<sub>2</sub>, and 50 mM KP<sub>i</sub> (pH 7.4) for 10 min at room temperature. Then, the samples were photoirradiated with a long wavelength UV lamp (Black Ray model B-100A, UVP, Upland, CA) for 10–20 min on ice, positioned 10 cm from the light source. The reaction was quenched by addition of 33  $\mu$ L of 4 $\times$  Laemmli- or Schgger-type sample buffer. When competition was examined, a competitor (other inhibitor) was added and the mixture incubated for 10 min at room temperature prior to the treatment with [<sup>125</sup>I]APF or [<sup>125</sup>I]AIF.

**Electrophoresis.** The labeled proteins in SMP were resolved by Laemmli- and Schgger-type SDS–PAGE according to standard procedures.<sup>26,27</sup> Analytical Blue Native (BN)-PAGE was performed using a Native PAGE Novex Bis-Tris Gel System with a 4 to 16% precast gel (Invitrogen, Carlsbad, CA). Visualization and quantification of the labeled proteins were conducted using Bioimaging Analyzer FLA-5100 (Fuji Film, Tokyo, Japan) and Multi gauge software (Fuji Film), respectively. Purification of complex I was performed by preparative BN-PAGE (5% isocratic gel) of the labeled SMP using 1% (w/v) DDM as a detergent.<sup>11</sup> The complex I band was identified by an activity stain and extracted by electroelution using Centrilotur (Millipore, Billerica, MA).

For the resolution of complex I components, doubled SDS–PAGE (dSDS–PAGE) was conducted as described by Rais et al.<sup>28</sup> Briefly, complex I subunits were separated on a first dimensional 10% Schgger-type gel (10% T, 3% C, containing 6 M urea). After acidification with 100 mM Tris-HCl (pH 2.0) for 30 min, the excised gel slice was subjected to second dimensional separation on a 16% Schgger-type gel (16% T, 3% C). Typically, complex I proteins equivalent to 300–500  $\mu$ g of SMP were separated on a mini-size gel format (80 mm  $\times$  90 mm  $\times$  1 mm). The resolved proteins were visualized by CBB or mass spectrometry (MS) compatible silver staining (Wako Silver stain MS kit, Wako Pure Chemicals, Osaka, Japan).

**Immunochemical Analysis.** The mobility of the PSST subunit on the SDS gel was profiled by Western blotting. Electrophoresed mitochondrial/complex I proteins were transferred onto a PVDF membrane (Immun-blot PVDF membrane, Bio-Rad) using the same conditions described previously.<sup>12,13</sup> The membrane was blocked with 1% gelatin in Tween TBS [0.9% NaCl, 0.05% Tween 20, and 10 mM Tris-HCl (pH 7.4)] for 1 h at room temperature. The blocked membrane was probed with the anti-*Paracoccus* Nqo6 (3000-fold dilution) for 1 h and then incubated for an additional 1 h with alkaline phosphatase-conjugated secondary antibody. The membrane was developed with an NBT/BCIP chromogenic substrate (AP-color development kit).

**Limited Proteolysis of the PSST and 49 kDa Subunits.** Partial digestion of the [<sup>125</sup>I]AIF-labeled 49 kDa subunit was conducted according to the procedure described in refs 15 and 29 using V8-protease and a 15% Tris-EDTA SDS–PAGE mapping gel. The V8 digestion was allowed to continue for 30 min to 1 h at room temperature. The digests were visualized by CBB staining and autoradiography. For exhaustive digestion of the labeled PSST and 49 kDa subunits, the labeled proteins were isolated by electroelution as described above and exhaustively digested using lysylendopeptidase (Lys-C, Wako Pure Chemicals, Osaka, Japan), endoprotease Asp-N (Loche,

Penzburg, Germany), or trypsin (Promega) in 50 mM Tris-HCl buffer (containing 0.1% SDS), 50 mM sodium phosphate buffer (containing 0.01% SDS), or ammonium bicarbonate buffer (containing 0.01% SDS), respectively.<sup>14</sup> The digests were analyzed by Tricine SDS–PAGE (16.5% T, 6% C).

**N-Terminal Amino Acid Sequence Analysis.** Protease digests of the 49 kDa subunit were identified by Edman degradation. They were transferred from the Tris-EDTA gel described above to PVDF membranes (Immobilon-P<sup>SQ</sup>, Millipore) in buffer containing 10 mM NaHCO<sub>3</sub>, 3 mM Na<sub>2</sub>CO<sub>3</sub>, and 0.025% (w/v) SDS overnight at 35 V (100 mA) in a cold room. The blotted membranes were stained with 0.025% CBB in 40% methanol and destained with 50% methanol. Bands were excised, and their N-terminal amino acid residues were identified with a Procise 494 HT Protein Sequencing System (Applied Biosystems, Foster City, CA) at the APRO Life Science Institute, Inc. (Tokushima, Japan).

**Mass Spectrometric Analysis.** Protein determination was conducted by MS. The [<sup>125</sup>I]APF- or [<sup>125</sup>I]AIF-labeled proteins were separated as a single band via SDS–PAGE (see Figures S2 and S3 of the Supporting Information), excised from the gel, destained, and treated with dithiothreitol and iodoacetamide. The proteins were in-gel digested with trypsin (Promega, Madison, WI) in a buffer containing 25 mM NH<sub>4</sub>HCO<sub>3</sub> at 37  $^{\circ}$ C overnight. After extraction of the digests from the gel using a solution containing 50% acetonitrile and 5% aqueous trifluoroacetic acid, they were concentrated to  $\sim$ 30  $\mu$ L and spotted onto a prespotted Anchor Chip (Bruker Daltonics, Billerica, MA) according to the manufacturer's protocol. Mass spectrometric analysis was conducted using a Bruker Autoflex III Smartbeam instrument (MALDI-TOF/TOF, Bruker Daltonics).

For peptide mass fingerprinting and MS/MS, peak detection and data processing were performed using flex Analysis and Biotools (Bruker Daltonics), respectively. The MS and MS/MS spectra were compared against SwissProt (<http://www.expasy.org/sprot>) using MASCOT (<http://matrixscience.com>), with a peptide mass tolerance of 150 ppm and a maximal missed cleavage of 1. Carbamidomethylation of cysteine residues and oxidation of methionine residues were set as variable modifications.

## RESULTS

**Synthesis and Characterization of APF and AIF.** Photoaffinity labeling is a powerful means of studying the interaction of biologically active chemicals with their target macromolecules.<sup>30</sup> For better analysis of the labeling experiments, it would be ideal if some photoreactive group could substitute for a pharmacophoric core structure with no loss of function, as discussed previously.<sup>15</sup> A structure–activity study of a series of fenpyroximate derivatives showed that the heterocyclic pyrazole ring including the 5-phenoxy group is a critical pharmacophoric core of the inhibitor, but the side chain part [the right side of the molecule (Figure 1)] has no specific function and contributes solely to an increase in the overall hydrophobicity of the molecule.<sup>31</sup> We designed therefore APF, which carries a photoreactive azido group on the 5-phenoxy group (Figure 1), to pinpoint the critical interaction between the pharmacophoric moiety and the enzyme. On the other hand, because [<sup>3</sup>H]TDF possesses a photoreactive group in the side chain part,<sup>10</sup> we also synthesized AIF to facilitate comparisons.



The inhibitory effect of the test compounds was examined with the NADH oxidase activity in SMP (30  $\mu$ g of protein/mL). The  $IC_{50}$  values of fenpyroximate, APF, and AIF were  $1.3 \pm 0.3$ ,  $2.3 \pm 0.6$ , and  $8.1 \pm 1.1$  nM, respectively, indicating that AIF is slightly less active (probably because of steric bulkiness) but still maintains a potent inhibitory effect at the nanomolar level. Thus, we chose APF and AIF as the photoaffinity labeling probes and synthesized their  $^{125}$ I-labeled derivatives [ $^{125}$ I]APF and [ $^{125}$ I]AIF, respectively (see the Supporting Information).

**Photoaffinity Labeling of SMP by [ $^{125}$ I]APF or [ $^{125}$ I]AIF.** UV irradiation of SMP (0.6 mg of protein/mL) in the presence of [ $^{125}$ I]APF (6 nM) gave two labeled protein bands and one labeled protein band at  $\sim 30$  and  $\sim 20$  kDa, respectively, on the 1D Tricine SDS–PAGE gel (10% T, 3% C) (Figure 2A). BN/

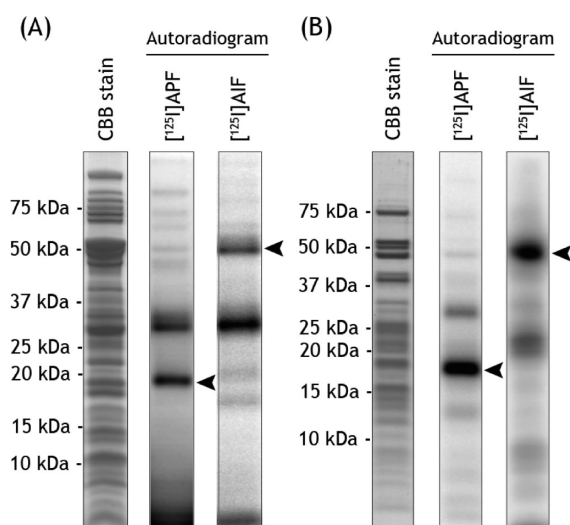


**Figure 2.** Photoaffinity labeling of bovine heart SMP by [ $^{125}$ I]APF or [ $^{125}$ I]AIF. (A) Bovine SMP (0.6 mg of protein/mL) were labeled with [ $^{125}$ I]APF or [ $^{125}$ I]AIF (6 nM each) in the presence of 50  $\mu$ M NADH. Proteins in SMP were separated on a Schgger-type Tricine gel (10% T, 3% C, containing 6 M urea) and autoradiographed. (B) [ $^{125}$ I]APF- or [ $^{125}$ I]AIF-labeled complex I was purified by preparative BN-PAGE as described in Experimental Procedures and analyzed on the 10% Schgger-type Tricine gel. An arrow indicates a major labeled protein in complex I.

SDS–PAGE analysis revealed that the two bands at  $\sim 30$  kDa represent the ADP/ATP carrier and 3-hydroxybutyrate dehydrogenase. After the complex I band had been isolated by electroelution from the BN–PAGE gel, the  $\sim 20$  kDa band appeared to be a major component of the labeled protein (Figure 2B), indicating that the  $\sim 20$  kDa protein houses the binding site of [ $^{125}$ I]APF.

The photoaffinity labeling by [ $^{125}$ I]AIF was performed by the same procedure. While [ $^{125}$ I]AIF also labeled the ADP/ATP carrier and 3-hydroxybutyrate dehydrogenase (Figure 2A), we detected major radioactivity in an  $\sim 50$  kDa protein (Figure 2B) after the complex I band had been isolated by electroelution from the BN–PAGE gel. Thus, our results strongly suggest that fenpyroximate binds to an interface formed by  $\sim 20$  and  $\sim 50$  kDa proteins. It should be noted that the labeling yield was considerably higher with [ $^{125}$ I]APF than with [ $^{125}$ I]AIF. This is probably because the pharmacophoric pyrazole moiety is recognized more strictly by the enzyme than the nonspecific side chain moiety. In addition, a good correlation was found between the labeling and the inhibition of NADH oxidase

activity for both [ $^{125}$ I]APF and [ $^{125}$ I]AIF (Figure S1 of the Supporting Information), indicating that the labeling by these probe chemicals is associated with the specific inhibition of complex I.

With regard to the labeling of both the ADP/ATP carrier and 3-hydroxybutyrate dehydrogenase by [ $^{125}$ I]APF and [ $^{125}$ I]AIF, we previously showed that the two proteins are also labeled by a quinazoline-type inhibitor, [ $^{125}$ I]AzQ, which also possesses the photoreactive azido-phenyl group, but the binding of [ $^{125}$ I]AzQ does not bring about dysfunction of the proteins.<sup>13</sup> The azido-phenyl group may have a high binding affinity for the proteins irrespective of differences in the inhibitor structure, though the reason remains to be elucidated. Identification of the binding site of the azido-phenyl group in the two proteins is currently underway in our laboratory.

Reaction yields of photolabeling and chemical labeling of complex I by various chemical reagents are sometimes enhanced by the treatment of the enzyme with NADH.<sup>10,15</sup> This was also the case for the labeling by [ $^{125}$ I]APF and [ $^{125}$ I]AIF; the radioactivity incorporated in the proteins was significantly improved (150–250%). Therefore, the photoaffinity labeling experiments described above and below were conducted in the presence of 50  $\mu$ M NADH. Moreover, in the previous labeling work with a quinazoline-type inhibitor,<sup>15</sup> we used an isolated bovine complex I to recover a sufficient amount of labeled protein. We did not use, however, the isolated enzyme in this study because the labeling yield with both [ $^{125}$ I]APF and [ $^{125}$ I]AIF was considerably poorer than that with SMP.

**Identification of the Labeled Subunits.** Complex I labeled with [ $^{125}$ I]APF was purified by preparative BN–PAGE and subjected to dSDS–PAGE analysis. This method is very effective for the separation of highly hydrophobic membrane proteins from water-soluble proteins and has been successfully employed to analyze integral membrane proteins such as mitochondrial respiratory complexes.<sup>32,33</sup> Notably, hydrophobic proteins in SMP are readily identified by their positions on the gel.<sup>32</sup> Our dSDS–PAGE patterns in the presence of 6 M urea seemingly agree with many published subunit compositions of purified complex I, in which each protein spot was identified by peptide mass fingerprinting (PMF).<sup>32,33</sup> By comparing them with known patterns, we could assign four hydrophobic spots, i.e., the ND5, ND4, ND2, and ND1 subunits (Figure 3A, left). Strong radioactivity was observed at a single spot in the dSDS gel (Figure 3A, right); the radioactivity in other regions was less than 5% of that of the spot. The position of this spot strongly suggests that the subunit labeled with [ $^{125}$ I]APF is the PSST, a central subunit housing the terminal iron–sulfur cluster N2 that acts as an immediate electron donor to ubiquinone.<sup>2,7</sup>

To verify this, we conducted Western blotting using an anti-bovine PSST antibody. The results showed that the radio-labeled protein is the PSST subunit (Figure S2 of the Supporting Information). However, PMF analysis of the in-gel tryptic digests of the radioactive spot indicated that it concomitantly contains the PGIV subunit. Therefore, we separated the PSST and PGIV subunits using a 16% Schgger-type Tricine gel (16% T, 6% C, containing 6 M urea) after the separation of complex I using a 10% Schgger-type Tricine gel (10% C, 3% T, containing 6 M urea) (Figure S3 of the Supporting Information) and again conducted a PMF analysis of the radioactive protein. The results confirmed the labeled protein to be the PSST subunit (Table S1 of the Supporting Information).

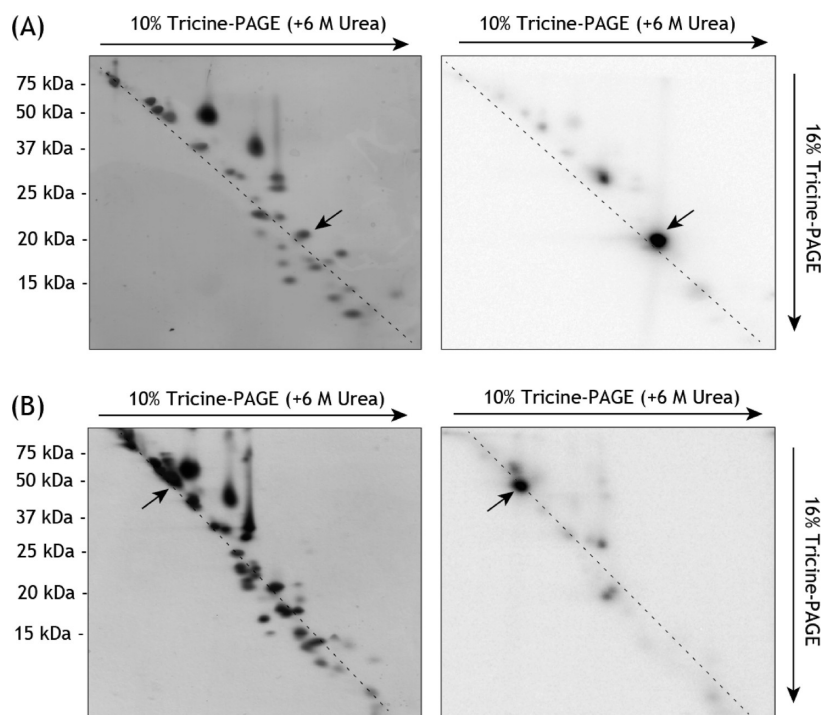


**Figure 3.** Resolution of the  $[^{125}\text{I}]\text{APF}$ - or  $[^{125}\text{I}]\text{AIF}$ -labeled complex I by dSDS-PAGE. (A) Complex I labeled with  $[^{125}\text{I}]\text{APF}$  (15 nM at 1.5 mg of protein/mL in the presence of 50  $\mu\text{M}$  NADH) was isolated by preparative BN-PAGE. The isolated complex I was separated on a 1D 10% Schagger-type Tricine gel (10% T, 3% C) followed by two-dimensional separation on a 16% Schagger-type gel (16% T, 3% C). Proteins were visualized by silver staining (left). The migration pattern of the labeled protein was monitored by autoradiography (right). (B) dSDS-PAGE analysis of complex I labeled with  $[^{125}\text{I}]\text{AIF}$  (15 nM at 1.5 mg of protein/mL in the presence of 50  $\mu\text{M}$  NADH). The labeled protein was profiled by silver staining (left) and autoradiography (right). Proteins labeled with  $[^{125}\text{I}]\text{APF}$  and  $[^{125}\text{I}]\text{AIF}$  (indicated by arrows) were identified to be the hydrophilic PSST and 49 kDa subunits, respectively.

Next, we analyzed the subunit labeled with  $[^{125}\text{I}]\text{AIF}$ . As shown in Figure 3B, the  $\sim 50$  kDa protein labeled with  $[^{125}\text{I}]\text{AIF}$  migrated to a single spot on the diagonal axis, not on the hydrophobic subunit spots. Although the 49 kDa subunit comigrated with the 51 kDa subunit in the dSDS-PAGE analysis, they could be separated as a single band on a 12.5% Laemmli-type gel (Figure S4 of the Supporting Information). The PMF analysis of the in-gel tryptic digests of the radioactive spot revealed that it is the 49 kDa subunit (Table S1 of the Supporting Information).

Altogether, our results unambiguously revealed that fenpyroximate binds to the interface between the hydrophilic PSST and 49 kDa subunits, not to the main body of the NDS subunit located at the distal end of the membrane domain, more than 100 Å from iron-sulfur cluster N2.

**Competition with Other Complex I Inhibitors.** Earlier photoaffinity labeling studies strongly suggested that structurally diverse complex I inhibitors share a large binding pocket composed of the hydrophilic 49 kDa/PSST and hydrophobic ND1 subunits.<sup>9,11–13</sup> We examined the effect of various complex I inhibitors (0.6  $\mu\text{M}$ , 100-fold excess) on the specific labeling of the PSST and 49 kDa subunits by  $[^{125}\text{I}]\text{APF}$  and  $[^{125}\text{I}]\text{AIF}$ , respectively. Figure 4 shows that an excess of fenpyroximate, bullatacin, aminoquinazoline, rotenone, or piericidin A almost completely suppressed the labeling. These results support the idea that fenpyroximate shares a common binding pocket with other inhibitors.

**Localization of the Labeled Site in the PSST Subunit.** The PSST subunit labeled with  $[^{125}\text{I}]\text{APF}$  was partially purified by preparative BN-PAGE and SDS-PAGE followed by

electroelution. When the PSST subunit was digested by Asp-N, Lys-C, or trypsin, a single radioactive band with an apparent molecular mass of  $\sim 8$ ,  $\sim 8$ , or  $\sim 3$  kDa, respectively, was obtained (Figure 5A). The Asp-N and Lys-C fragments, which

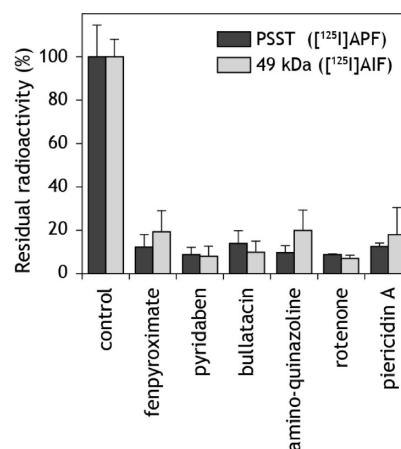


**Figure 4.** Effect of various complex I inhibitors on the specific labeling of the PSST and 49 kDa subunits. SMP (0.6 mg of protein/mL) were labeled with 6 nM  $[^{125}\text{I}]\text{APF}$  or  $[^{125}\text{I}]\text{AIF}$  in the presence of 50  $\mu\text{M}$  NADH and various complex I inhibitors at 0.6  $\mu\text{M}$  (100-fold). The labeled SMP were analyzed on a 10% Schagger-type Tricine gel (10% T, 3% C, containing 6 M urea), and the residual radioactivity in the PSST and 49 kDa subunits was quantified. The averaged control radioactivity in the PSST and 49 kDa subunits was  $\sim 800$  and  $\sim 300$  cpm, respectively. Data are the means of three independent experiments  $\pm$  the standard deviation.

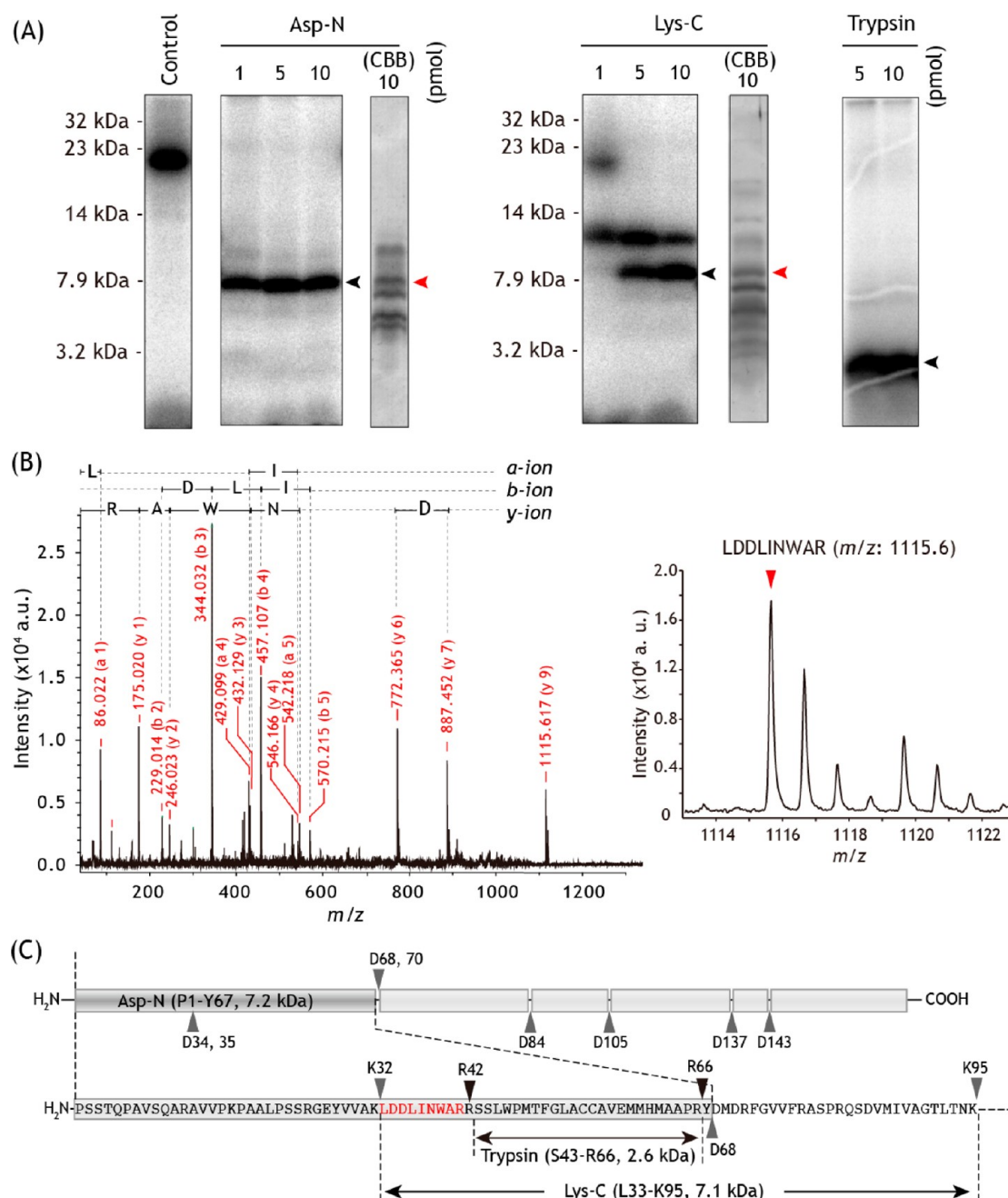


**Figure 5.** Localization of the [ $^{125}$ I]APF-labeled site in the PSST subunit. (A) The [ $^{125}$ I]APF-labeled PSST subunit was partially purified by preparative BN-PAGE and SDS-PAGE on a 10% Schagger-type Tricine gel (10% T, 3% C, containing 6 M urea). The isolated PSST subunit was digested by Asp-N, Lys-C, or trypsin according to a procedure described previously.<sup>15</sup> The proteolytic digests were analyzed on a 16% Schagger-type Tricine gel (16% T, 6% C, containing 6 M urea). The amounts of proteases in the reaction buffer are indicated on the top of each autoradiogram. The CBB-stained Asp-N or Lys-C fragment (equivalent to 2 mg of SMP protein/lane), corresponding to the converged radioactivity, is denoted with a red arrow. (B) The labeled Asp-N and Lys-C fragments were subjected to in-gel tryptic digestion. MALDI-TOF MS analysis of the tryptic digests revealed that both fragments contain the same peptide ( $m/z$  1115.6, right), which could be assigned as peptide L<sup>33</sup>DDLINWAR<sup>41</sup> by MS/MS (left). (C) Schematic presentation of the digestion of the PSST subunit by Asp-N, Lys-C, or trypsin. The residue numbers of the predicted cleavage sites refer to the mature sequence of the bovine PSST subunit (SwissProt entry P42026) after the removal of the transit peptide to the mitochondrion.

correspond to the radioactive bands in the autoradiogram, were detected by CBB staining (Figure 5A). By MS and MS/MS analyses of the Asp-N fragment, we identified a tryptic fragment, L<sup>33</sup>DDLINWAR<sup>41</sup> [ $m/z$  1115.6 (Figure 5B)]. Considering this partial sequence and its apparent molecular mass, the Asp-N fragment appeared to be peptide Pro1–Tyr67 (7.2 kDa) containing two uncleavable Asp residues (D<sup>34</sup>D<sup>35</sup>). We also detected the same tryptic fragment, L<sup>33</sup>DDLINWAR<sup>41</sup>,

only from the radioactive Lys-C fragment (Figure 5A). This result strongly suggests that the Lys-C fragment is peptide Leu33–Lys95 (7.1 kDa). It is therefore likely that the radioactive tryptic fragment of the labeled PSST subunit is peptide Ser43–Arg66 (2.6 kDa, 24 amino acids), which is located in the N-terminal region of the subunit. These results are summarized in Figure 5C.



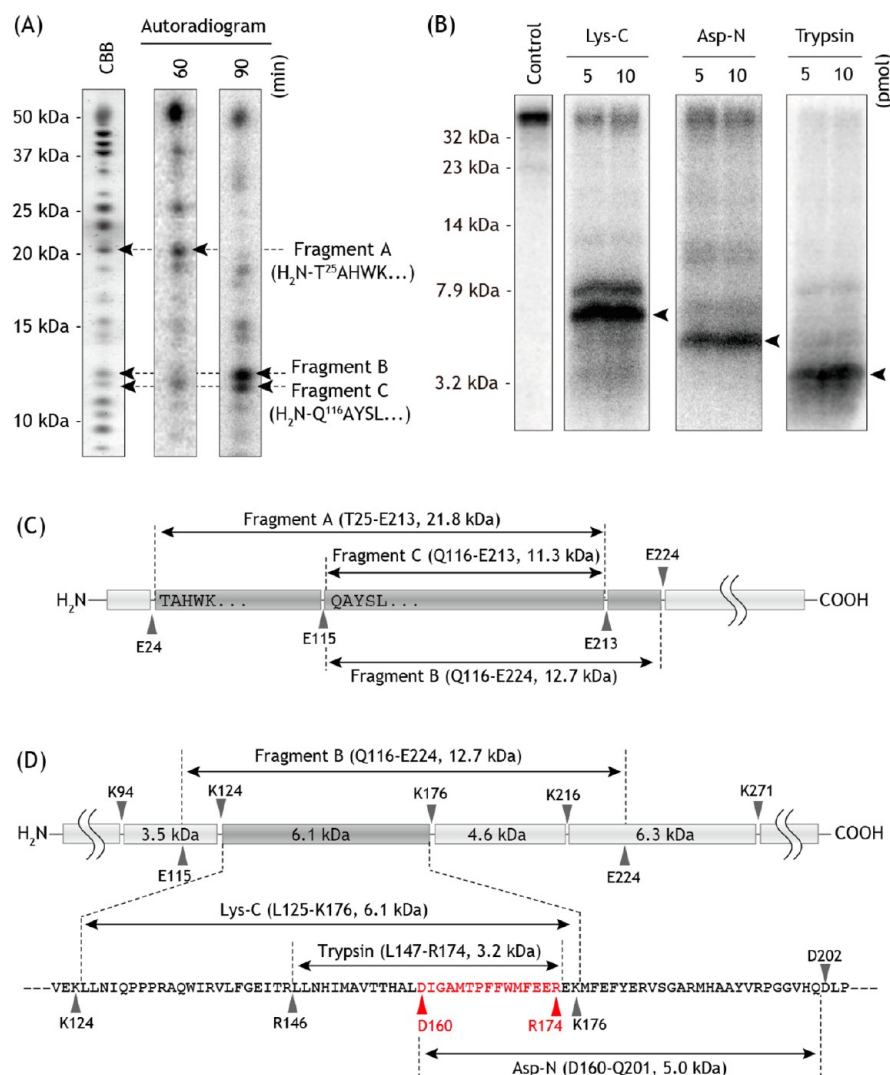


**Figure 6.** Localization of the [ $^{125}\text{I}$ ]AIF-labeled site in the 49 kDa subunit. The [ $^{125}\text{I}$ ]AIF-labeled 49 kDa subunit was purified by preparative BN-PAGE and SDS-PAGE on a 12.5% Laemmli-type gel. (A) The CBB-stained gel piece of the 49 kDa subunit was subjected to partial digestion by V8-protease (60 or 90 min) as described in Experimental Procedures. The radioactive bands (fragments A–C) were analyzed by N-terminal sequencing. (B) The [ $^{125}\text{I}$ ]AIF-labeled 49 kDa subunit was digested exhaustively with Lys-C, Asp-N, or trypsin. Each digest was analyzed on a 16% Schagger-type Tricine gel (16% T, 6% C, containing 6 M urea). The amounts of proteases in the reaction buffer are indicated at the top of each autoradiogram. (C) Schematic presentation of the partial digestion of the 49 kDa subunit by V8-protease. The predicted cleavage sites are denoted with arrows and indicated by their residue numbers in the mature sequence of the 49 kDa subunit (SwissProt entry P17694). (D) Schematic presentation of the exhaustive digestion of the 49 kDa subunit by Lys-C, Asp-N, or trypsin in the region covering fragment B (Gln116–Glu224). The [ $^{125}\text{I}$ ]AIF-labeled region (Asp160–Arg174) is colored red.

**Localization of the Labeled Site in the 49 kDa Subunit.** We conducted partial digestion of the [ $^{125}\text{I}$ ]AIF-labeled 49 kDa subunit by V8-protease to roughly localize the labeled region in the subunit, whose molecular mass is more than twice that of the PSST subunit. The digestion reproducibly gave several radioactive bands on a 15% Tris-EDTA SDS-PAGE mapping gel (Figure 6A), which converged on ~13 kDa bands [fragments B and C (Figure 6A)]. By MS and MS/MS analyses of fragments A–C, we detected a tryptic fragment  $\text{M}^{177}\text{FEFYER}^{183}$  [ $m/z$  1021.5 or 1037.5 (for the Met-oxidized peptide)] in common. The N-terminal sequence of fragments B and C, transferred onto a PVDF membrane, was determined to be  $\text{H}_2\text{N}-\text{Q}^{116}\text{ASYL}$ , indicating that the former and latter are the Gln116–Glu224 and Gln116–Glu213 regions, respectively (Figure 6C). Taking into consideration the fact that the N-terminal sequence of fragment A was

determined to be  $\text{H}_2\text{N}-\text{T}^{25}\text{AHWK}$ , we find that [ $^{125}\text{I}$ ]AIF labels the Gln116–Glu213 region.

Next, the [ $^{125}\text{I}$ ]AIF-labeled 49 kDa subunit was subjected to exhaustive digestion by Lys-C, Asp-N, and trypsin, with major radioactive bands observed at ~6, ~5, and ~3 kDa, respectively (Figure 6B). Careful examination of the predicted cleavage sites for these proteases in the region determined by the V8-protease partial digestion (Gln116–Glu213) strongly suggested that the Lys-C, Asp-N, and tryptic fragments are peptides Lys125–Lys176 (6.1 kDa), Asp160–Gln201 (5.0 kDa), and Leu147–Arg174 (3.2 kDa), respectively. Taken together, the [ $^{125}\text{I}$ ]AIF-labeled residue in the 49 kDa subunit is located in the Asp160–Arg174 region [15 amino acids (Figure 6D)].

To attempt to pinpoint the amino acid residue(s) labeled by [ $^{125}\text{I}$ ]ABF or [ $^{125}\text{I}$ ]AIF, we conducted PMF analyses of the labeled subunits. However, the labeled peptides (and a photoproduct of the inhibitor) discussed here could not be

readily detected because of the low yield of the labeling reaction (~5%).<sup>15</sup>

## DISCUSSION

Our results unambiguously revealed that fenpyroximate does not bind to the main body of the ND5 subunit located at the distal end of the membrane domain but rather resides at the interfacial region between the hydrophilic and membrane domains in a manner such that the pharmacophoric pyrazole ring and side chain of the inhibitor orient toward the PSST and 49 kDa subunits, respectively. This result seems to be consistent with an earlier photoaffinity study by Schuler et al.,<sup>9</sup> demonstrating that a pyridaben derivative, which is similar in structure to fenpyroximate,<sup>34</sup> binds to the PSST subunit. The crystal structure of complex I from *T. thermophilus* revealed that a high-potential Fe–S cluster N2 is located near the cavity between subunits Nqo4 and Nqo6 (49 kDa and PSST in bovine), which forms part of a large cavity at the interface of these subunits with hydrophobic subunit Nqo8 (ND1) and the Nqo7/10/11 (ND3/6/4L) bundle.<sup>5</sup> The cavity at the interface of subunits Nqo4, Nqo6, and Nqo8 and the Nqo7/10/11 bundle is thought to provide a common binding domain for quinone and various inhibitors,<sup>5,9,13–17</sup> though the architecture of this cavity has not yet been completely resolved.<sup>5</sup> It is worth noting that on the basis of the structural model of *T. thermophilus* complex I,<sup>5</sup> the labeled regions identified in this study [Ser43–Arg66 (PSST) and Asp160–Arg174 (49 kDa)], which correspond to Asn34–Arg57 (Nqo6) and Asp139–Arg153 (Nqo4), respectively, face this cavity (Figure 7). The region labeled by the quinazoline-type inhibitor in the 49 kDa subunit<sup>15</sup> [Asp41–Arg63 in bovine, which is resolved in the crystal structure (Met26–Gly31 and Gly39–Arg42 in Nqo4)] is also shown in Figure 7B (light blue spheres). Given that acetogenin binds to the third matrix side loop of the ND1 subunit,<sup>35,36</sup> chemically diverse inhibitors bind to the cavity, but in considerably different manners depending upon their chemical properties.

Nakamaru-Ogiso et al.<sup>10</sup> reported that a fenpyroximate derivative ([<sup>3</sup>H]TDF) binds to the ND5 subunit, though the labeled region in the subunit was not identified. It has now been established that the body of the ND5 subunit is located at the distal (from the hydrophilic domain) end of the membrane domain.<sup>5</sup> How can we explain the contradictory results for the binding of fenpyroximate between the earlier study<sup>10</sup> and this research? Although the current structural model of complex I is incomplete in the interfacial region,<sup>5</sup> several experiments using cross-linking reagents may provide a clue about this point. Using *Paracoccus denitrificans* membrane preparations, Kao et al. demonstrated that the Nqo4 (49 kDa) and Nqo6 (PSST) subunits are cross-linked to the Nqo7 (ND3) subunit by a zero-length cross-linker, indicating direct interaction between the subunits.<sup>37</sup> Galkin et al. suggested that the loop between the first and second transmembrane helices of the ND3 subunit in bovine complex I is part of the structure connecting the peripheral and membrane domains.<sup>32</sup> It is therefore likely that some segments of the 49 kDa and PSST subunits are in close contact with the ND3/ND6/ND4L bundle in the membrane domain. In addition, the crystal structure of *T. thermophilus* complex I<sup>5</sup> showed that the 16th TM helix of Nqo12 (ND5 in bovine), which extends from the body of the subunit, resides in the vicinity of the Nqo7/10/11 bundle. Altogether, the results reported by Nakamaru-Ogiso et al. would be explained if we suppose that a segment of the ND5 subunit, which corresponds

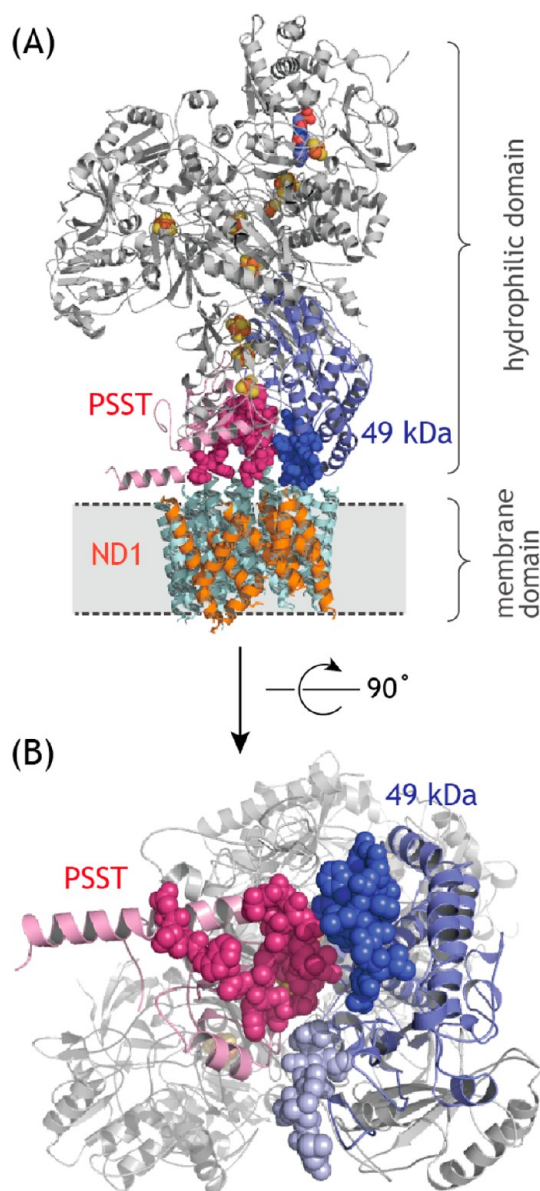


**Figure 7.** Structure of the hydrophilic domain and the ND1 subunit revealed from the structural model of *T. thermophilus* complex I (PDB entry 3M9S<sup>5</sup>). (A) The Nqo6 (the bacterial homologue of the PSST subunit), Nqo4 (49 kDa), and Nqo8 (ND1) subunits are colored in magenta, blue, and orange, respectively. Using a sequence alignment for the bovine PSST and 49 kDa subunits and *T. thermophilus* Nqo6 and Nqo4 (Figures S5 and S6 of the Supporting Information), respectively, the labeled sections identified here are represented with spheres. (B) Close-up view from the periplasmic side (rotated by 90°). The membrane domain was omitted to show the “quinone-binding cavity”. For comparison, the region labeled by the quinazoline-type inhibitor in the 49 kDa subunit<sup>15</sup> is represented with light blue spheres.

to the 16th TM helix of *T. thermophilus* Nqo12, is located close to the interface with the hydrophilic domain (especially the 49 kDa subunit) in the bovine enzyme and that the photoreactive diazirine group of [<sup>3</sup>H]TDF labeled this segment. The fact that [<sup>3</sup>H]TDF also labeled the 49 kDa subunit with a frequency of ~1:4 (49 kDa:ND1)<sup>10</sup> might support this speculation. The crystal structure<sup>5</sup> revealed that the 16th TM helix does not reach the contact region with the hydrophilic domain. However, given that the ND2 subunit in the bovine enzyme



is significantly shorter (~100 amino acids) than its counterpart in *T. thermophilus*,<sup>38</sup> it is possible that the position of the 16th TM helix in the membrane domain is somewhat different between the two enzymes. Regardless, it is important to stress that fenpyroximate does not bind to the body of the ND5 subunit located at the distal end of the membrane domain. We note that our conclusion does not argue against the significant functional role of the ND5 subunit in the proton translocation suggested by the X-ray crystal structure<sup>5</sup> and mutagenesis studies.<sup>20,39,40</sup>

To determine the function of the membrane domain, it is important to clarify whether there is an additional binding site for quinone and/or inhibitors besides the interfacial region of the PSST, 49 kDa, and ND1 subunits.<sup>2,7</sup> Photoaffinity labeling studies conducted by other research groups suggested the presence of such an additional site in the membrane domain. For instance, a photoaffinity labeling experiment using [<sup>3</sup>H]azidoquinone suggested that the NuoM subunit of *E. coli* complex I (ND4 in bovine) houses the ubiquinone binding site.<sup>41</sup> However, it should be noted that [<sup>3</sup>H]azidoquinone did not bind to the interfacial region connecting the PSST, 49 kDa, and ND1 subunits and that their mass spectrometry-based identification of the peptide fragment labeled with [<sup>3</sup>H]-azidoquinone (i.e., the Val184–Asn206 region in the NuoM subunit with a photoproduct of [<sup>3</sup>H]azidoquinone) was later questioned.<sup>42</sup> It seems to be difficult, in our view, to conduct accurate MS analysis of the cross-linked peptide in ref 41 because of significant contamination by unknown peptides in the most radioactive fraction (see the HPLC chromatogram shown in Figure 5 of ref 41). Additionally, while His196 was suggested to be involved in quinone binding,<sup>41</sup> the mutation of this residue did not significantly affect the characteristics of the enzyme.<sup>43</sup>

Furthermore, Nakamaru-Ogiso et al.<sup>19</sup> recently argued that a photoreactive derivative of asimicin ([<sup>3</sup>H]BPA), a member of the group of natural acetogenins, concomitantly labeled three subunits, the ND1, ND2, and ND5 subunits. Judging from the labeling profiles shown in ref 19, however, the results seem questionable because the specificity of the labeling against both complex I (among another respiratory complexes) and these subunits is not so high. The low specificity may be associated with the physicochemical properties of [<sup>3</sup>H]BPA as follows. First, given that no specific structural factor of the alkyl side chain of acetogenins is required for binding to the enzyme,<sup>44–46</sup> the long alkyl chain of [<sup>3</sup>H]BPA, to which a photoreactive benzophenone group was attached, is too flexible to fix the position of benzophenone in the enzyme. Second, it should be realized that while a photoreactive benzophenone group is thought to exhibit a high photo-cross-linking yield, this is because a benzophenone is activated by UV irradiation in a reversible manner via excitation (an excited triplet state)—relaxation cycles;<sup>30</sup> in other words, a benzophenone is not photolabile by UV irradiation unlike diazirine and azido groups. These properties of [<sup>3</sup>H]BPA together would enhance the probability of nonspecific labeling at the bound state. We recently revealed that both of two pharmacophoric components of natural acetogenins (i.e., the terminal  $\gamma$ -lactone ring and the hydroxylated bis-THF ring) bind to the ND1 subunit with high specificity.<sup>35,36</sup>

In general, as the photoaffinity labeling largely depends upon both physicochemical and biological capabilities of the probe molecule and is prone to give false positive results, especially due to nonspecific labeling,<sup>30</sup> the results must be carefully

interpreted, as discussed in refs 7 and 13. On the basis of the crystal structure of the membrane domain of *E. coli*,<sup>24</sup> there is no strong evidence forcing us to accept a scenario more complicated than that of a single functional site where ubiquinone reduction couples to proton translocation through long-range conformational changes.<sup>7,47</sup>

In conclusion, to clarify the binding site of fenpyroximate, we reinvestigated the photoaffinity labeling experiment using newly synthesized fenpyroximate derivatives [<sup>125</sup>I]APF and [<sup>125</sup>I]AIF. Our results unambiguously reveal that fenpyroximate does not bind to the body of the ND5 subunit located at the distal end of the membrane domain but rather resides at the interface between the PSST and 49 kDa subunits with high specificity. This study resolves a critical issue relating to complex I, improving our knowledge of the function of the membrane domain.

## ■ ASSOCIATED CONTENT

### ■ Supporting Information

Synthesis of [<sup>125</sup>I]APF and [<sup>125</sup>I]AIF, Table S1, and Figures S1–S6. This material is available free of charge via the Internet at <http://pubs.acs.org>.

## ■ AUTHOR INFORMATION

### Corresponding Author

\*E-mail: [miyoshi@kais.kyoto-u.ac.jp](mailto:miyoshi@kais.kyoto-u.ac.jp). Telephone: +81-75-753-6119. Fax: +81-75-753-6408.

### Funding

This work was supported by a Grant-in-aid for Scientific Research (Grant 23380064 to H.M.) and a Grant-in-aid for Young Scientists (Grant 23780116 to M.M.) from the Japan Society for the Promotion of Science.

### Notes

The authors declare no competing financial interest.

## ■ ABBREVIATIONS

AIF, 3-azido-5-iodobenzyl fenpyroximate; [<sup>125</sup>I]AIF, <sup>125</sup>I-labeled AIF; APF, 4-azidophenyl fenpyroximate; [<sup>125</sup>I]APF, <sup>125</sup>I-labeled APF; CBB, Coomassie brilliant blue R250; complex I, proton-translocating NADH-quinone oxidoreductase; MALDI-TOF, matrix-assisted laser desorption/ionization time-of-flight; MS, mass spectrometry; PMF, peptide mass fingerprinting; PVDF, polyvinylidene fluoride; SDS–PAGE, sodium dodecyl sulfate–polyacrylamide gel electrophoresis; dSDS–PAGE, doubled SDS–PAGE; SMP, submitochondrial particles; TM, transmembrane.

## ■ REFERENCES

- (1) Brandt, U. (2006) Energy converting NADH:quinone oxidoreductase (complex I). *Annu. Rev. Biochem.* 75, 69–92.
- (2) Hirst, J. (2010) Towards the molecular mechanism of respiratory complex I. *Biochem. J.* 425, 327–339.
- (3) Carroll, J., Fearnley, I. M., Skehel, J. M., Shannon, R. J., Hirst, J., and Walker, J. E. (2006) Bovine complex I is a complex of 45 different subunits. *J. Biol. Chem.* 281, 32724–32727.
- (4) Sazanov, L. A., and Hinchliffe, P. (2006) Structure of the hydrophilic domain of respiratory complex I from *Thermus thermophilus*. *Science* 311, 1430–1436.
- (5) Efremov, R. G., Baradaran, R., and Sazanov, L. A. (2010) The architecture of respiratory complex I. *Nature* 465, 441–445.
- (6) Hunte, C., Zickermann, V., and Brandt, U. (2010) Functional modules and structural basis of conformational coupling in mitochondrial complex I. *Science* 329, 448–451.

- (7) Tocilescu, M. A., Zickermann, V., Zwicker, K., and Brandt, U. (2010) Quinone binding and reduction by respiratory complex I. *Biochim. Biophys. Acta* 1797, 1883–1890.
- (8) Earley, F. G. P., Patel, S. D., Ragan, C. I., and Attardi, G. (1987) Photolabeling of a mitochondrially encoded subunit of NADH dehydrogenase with [<sup>3</sup>H]dihydrorotenone. *FEBS Lett.* 219, 108–113.
- (9) Schuler, F., Yano, T., Bernardo, S. D., Yagi, T., Yankovskaya, V., Singer, T. P., and Casida, J. E. (1999) NADH-quinone oxidoreductase: PSST subunit couples electron transfer from iron-sulfur cluster N2 to quinone. *Proc. Natl. Acad. Sci. U.S.A.* 96, 4149–4153.
- (10) Nakamaru-Ogiso, E., Sakamoto, K., Matsuno-Yagi, A., Miyoshi, H., and Yagi, T. (2003) The ND5 subunit was labeled by a photoaffinity analogue of fenpyroximate in bovine mitochondrial complex I. *Biochemistry* 42, 746–754.
- (11) Murai, M., Ishihara, A., Nishioka, T., Yagi, T., and Miyoshi, H. (2007) The ND1 subunit constructs the inhibitor binding domain in bovine heart mitochondrial complex I. *Biochemistry* 46, 6409–6416.
- (12) Ichimaru, N., Murai, M., Kakutani, N., Kako, J., Ishihara, A., Nakagawa, Y., Nishioka, T., Yagi, T., and Miyoshi, H. (2008) Synthesis and characterization of new piperazine-type inhibitors for mitochondrial NADH-ubiquinone oxidoreductase (complex I). *Biochemistry* 47, 10816–10826.
- (13) Murai, M., Sekiguchi, K., Nishioka, T., and Miyoshi, H. (2009) Characterization of the inhibitor binding site in mitochondrial NADH-ubiquinone oxidoreductase by photoaffinity labeling using a quinazoline-type inhibitor. *Biochemistry* 48, 688–698.
- (14) Kakutani, N., Murai, M., Sakiyama, N., and Miyoshi, H. (2010) Exploring the binding site of  $\Delta$ lac-acetogenin in bovine heart mitochondrial NADH-ubiquinone oxidoreductase. *Biochemistry* 49, 4794–4803.
- (15) Murai, M., Mashimo, Y., Hirst, J., and Miyoshi, H. (2011) Exploring interactions between the 49 kDa and ND1 subunits in mitochondrial NADH-ubiquinone oxidoreductase (complex I) by photoaffinity labeling. *Biochemistry* 50, 6901–6908.
- (16) Tocilescu, M. A., Fendel, U., Zwicker, K., Kerscher, S., and Brandt, U. (2007) Exploring the ubiquinone binding cavity of respiratory complex I. *J. Biol. Chem.* 282, 29514–29520.
- (17) Fendel, U., Tocilescu, M. A., Kerscher, S., and Brandt, U. (2008) Exploring the inhibitor binding pocket of respiratory complex I. *Biochim. Biophys. Acta* 1777, 660–665.
- (18) Okun, J. G., Lümmer, P., and Brandt, U. (1999) Three classes of inhibitor share a common binding domain in mitochondrial complex I (NADH-ubiquinone oxidoreductase). *J. Biol. Chem.* 274, 2625–2630.
- (19) Nakamaru-Ogiso, E., Han, H., Matsuno-Yagi, A., Keinan, E., Sinha, S. C., Yagi, T., and Ohnishi, T. (2010) The ND2 subunit is labeled by a photoaffinity analogue of asimicin, a potent complex I inhibitor. *FEBS Lett.* 584, 883–888.
- (20) Nakamaru-Ogiso, E., Kao, M.-C., Chen, H., Sinha, S. C., Yagi, T., and Ohnishi, T. (2010) The membrane subunit NuoL (ND5) is involved in the indirect proton pumping mechanism of *Escherichia coli* complex I. *J. Biol. Chem.* 285, 39070–39078.
- (21) Batista, A. P., Marreiros, B. C., and Pereira, M. M. (2011) Decoupling of catalytic transport activities of *Rhodothermus marinus* complex I by a sodium/proton antiporter inhibitor. *ACS Chem. Biol.* 6, 477–483.
- (22) Moparthi, V. K., Kumar, B., Mathiesen, C., and Hägerhäll, C. (2011) Homologous protein subunits from *Escherichia coli* NADH-quinone oxidoreductase can functionally replace MrpA and MrpD in *Bacillus subtilis*. *Biochim. Biophys. Acta* 1807, 427–436.
- (23) Michel, J., Deleon-Rangel, J., Zhu, S., Van Ree, K., and Vik, S. B. (2011) Mutagenesis of the L, M, and N subunits of complex I from *Escherichia coli* indicates a common role in function. *PLoS One* 6, e17420.
- (24) Efremov, R. G., and Sazanov, L. A. (2011) Structure of the membrane domain of respiratory complex I. *Nature* 476, 414–420.
- (25) Matsuno-Yagi, A., and Hatefi, Y. (1985) Studies on the mechanism of oxidative phosphorylation. *J. Biol. Chem.* 260, 14424–14427.
- (26) Laemmli, U. K. (1970) Cleavage of structural proteins during the assembly of the head of bacteriophage T4. *Nature* 227, 680–685.
- (27) Schägger, H. (2006) Tricine-SDS-PAGE. *Nat. Protoc.* 1, 16–21.
- (28) Rais, I., Kara, M., and Schägger, H. (2004) Two-dimensional electrophoresis for the isolation of integral membrane proteins and mass spectrometric identification. *Proteomics* 4, 2567–2571.
- (29) Cleveland, D. W., Fishcher, M. W., Kirschner, M. W., and Laemmli, U. K. (1977) Peptide mapping by limited proteolysis in sodium dodecyl sulfate and analysis by gel electrophoresis. *J. Biol. Chem.* 252, 1102–1106.
- (30) Kotzyba-Hibert, F., Kapfer, I., and Goeldner, M. (1995) Recent trends in photoaffinity labeling. *Angew. Chem., Int. Ed.* 34, 1296–1312.
- (31) Hamaguchi, H., Kajihara, O., and Katoh, M. (1995) Development of acaricide fenpyroximate. *J. Pestic. Sci.* 20, 203–212.
- (32) Galkin, A., Meyer, B., Wittig, I., Karas, M., Schägger, H., Vinogradov, A., and Brandt, U. (2008) Identification of the mitochondrial ND3 subunit as a structural component involved in the active/deactive enzyme transition of respiratory complex I. *J. Biol. Chem.* 283, 20907–20913.
- (33) Adbrakmanova, A., Zickermann, V., Bostina, M., Radermacher, M., Shägger, H., Kerscher, S., and Brandt, U. (2004) Subunit composition of mitochondrial complex I from the yeast *Yarrowia lipolytica*. *Biochim. Biophys. Acta* 1658, 148–156.
- (34) Akagi, T., Takahashi, Y., and Sasaki, S. (1996) Exhaustive conformational searches for superimposition of acaricidal compounds. *Quantitative Structure-Activity Relationships* 15, 290–295.
- (35) Sekiguchi, K., Murai, M., and Miyoshi, H. (2009) Exploring the binding site of acetogenin in the ND1 subunit of bovine mitochondrial complex I. *Biochim. Biophys. Acta* 1787, 1106–1111.
- (36) Nakanishi, S., Abe, M., Yamamoto, S., Murai, M., and Miyoshi, H. (2011) Bis-THF motif of acetogenin binds to the third matrix-side loop of ND1 subunit in mitochondrial NADH-ubiquinone oxidoreductase. *Biochim. Biophys. Acta* 1807, 1170–1176.
- (37) Kao, M.-C., Matsuno-Yagi, A., and Yagi, T. (2004) Subunit proximity in the H<sup>+</sup>-translocating NADH-quinone oxidoreductase probed by zero-length cross-linking. *Biochemistry* 43, 3750–3755.
- (38) Birrell, J. A., and Hirst, J. (2010) Truncation of subunit ND2 disrupts the threefold symmetry of the antiporter-like subunits in complex I from higher metazoans. *FEBS Lett.* 584, 4247–4252.
- (39) Steimle, S., Bajzath, C., Dorner, K., Schulte, M., Bothe, V., and Friedrich, T. (2011) Role of subunit NuoL for proton translocation by respiratory complex I. *Biochemistry* 50, 3386–3393.
- (40) Oröse, S., Krack, S., Sokolova, L., Zwicker, K., Barth, H.-D., Morgner, N., Heide, H., Steger, M., Nübel, E., Zickermann, V., Kerscher, S., Brutschy, B., Radermacher, M., and Brandt, U. (2011) Functional dissection of the proton pumping modules of mitochondrial complex I. *PLoS Biol.* 9, e1001128.
- (41) Gong, X., Xie, T., Yu, L., Hesterberg, M., Scheide, D., Friedrich, T., and Yu, C.-A. (2003) The ubiquinone-binding site in NADH-ubiquinone oxidoreductase from *Escherichia coli*. *J. Biol. Chem.* 278, 25731–25737.
- (42) Matsumoto, Y., Murai, M., Fujita, D., Sakamoto, K., Miyoshi, H., Yoshida, M., and Mogi, T. (2006) Mass spectrometric analysis of the ubiquinol-binding site in cytochrome *bd* from *Escherichia coli*. *J. Biol. Chem.* 281, 1905–1912.
- (43) Torres-Bacete, J., Nakamaru-Ogiso, E., Matsuno-Yagi, A., and Yagi, T. (2007) Characterization of the NuoM (ND4) subunit in *Escherichia coli* NDH-1: Conserved charged residues essential for energy-coupled activities. *J. Biol. Chem.* 282, 36914–36922.
- (44) Motoyama, T., Yabunaka, H., and Miyoshi, H. (2002) Essential structural factors of acetogenins, potent inhibitors of mitochondrial complex I. *Bioorg. Med. Chem. Lett.* 12, 2089–2092.
- (45) Abe, M., Murai, M., Ichimaru, N., Kenmochi, A., Yoshida, T., Kubo, A., Kimura, Y., Moroda, A., Makabe, H., Nishioka, T., and Miyoshi, H. (2005) Dynamic function of the alkyl spacer of acetogenins in their inhibitory action with mitochondrial complex I (NADH-ubiquinone oxidoreductase). *Biochemistry* 44, 14898–14906.
- (46) Abe, M., Kubo, A., Yamamoto, S., Hatoh, Y., Murai, M., Hattori, Y., Makabe, H., Nishioka, T., and Miyoshi, H. (2008) Dynamic

function of the spacer region of acetogenins in the inhibition of bovine mitochondrial NADH-ubiquinone oxidoreductase (complex I). *Biochemistry* 47, 6260–6266.

(47) Brandt, U. (2011) A two-state stabilization-change mechanism for proton-pumping complex I. *Biochim. Biophys. Acta* 1807, 1364–1369.